Published in final edited form as:

Cancer Lett. 2017 August 28; 402: 177–189. doi:10.1016/j.canlet.2017.05.028.

Suppression of Akt1- β-catenin pathway in advanced prostate cancer promotes TGFβ1-mediated epithelial to mesenchymal transition and metastasis

Fei Gao[1,2], **Abdulrahman Alwhaibi**[1], **Harika Sabbineni**[1], **Arti Verma**[1], **Wael Eldahshan**[1], and **Payaningal R. Somanath**[1,3,*]

[1]Clinical and Experimental Therapeutics, College of Pharmacy, University of Georgia and Charlie Norwood VA Medical Center, Augusta, GA 30912

[2]Department of Urology, The First Affiliated Hospital of Chongqing Medical University, Chongqing, China

[3]Department of Medicine, Vascular Biology Center and Cancer Center, Augusta University, Augusta, GA 30912

Abstract

Akt1 is essential for the oncogenic transformation and tumor growth in various cancers. However, the precise role of Akt1 in advanced cancers is conflicting. Using a neuroendocrine TRansgenic Adenocarcinoma of the Mouse Prostate (*TRAMP*) model, we first show that the genetic ablation or pharmacological inhibition of Akt1 in mice blunts oncogenic transformation and prostate cancer (PCa) growth. Intriguingly, triciribine (TCBN)-mediated Akt inhibition in 25-week old, tumor-bearing *TRAMP* mice and Akt1 gene silencing in aggressive PCa cells enhanced epithelial to mesenchymal transition (EMT) and promoted metastasis to the lungs. Mechanistically, Akt1 suppression leads to increased expression of EMT markers such as Snail1 and N-cadherin and decreased expression of epithelial marker E-cadherin in *TRAMP* prostate, and in PC3 and DU145 cells. Next, we identified that Akt1 knockdown in PCa cells results in increased production of TGFβ1 and its receptor TGFβ RII, associated with a decreased expression of β-catenin. Furthermore, treatment of PCa cells with ICG001 that blocks nuclear translocation of β-catenin promoted EMT and N-cadherin expression. Together, our study demonstrates a novel role of the Akt1-β-catenin-TGFβ1 pathway in advanced PCa.

Keywords

Akt1; β-catenin; prostate cancer; epithelial-to-mesenchymal transition; metastasis

*Corresponding author: Payaningal R. Somanath, Ph.D., FAHA., Associate Professor, Clinical and Experimental Therapeutics, College of Pharmacy, University of Georgia, HM1200 – Augusta University, Augusta, GA 30912., Phone: 706-721-4250; Fax: 706-721-3994; sshenoy@augusta.edu.

Conflict of interest: Authors declare that there are no financial or conflicts of interests exist.

1. Introduction

Despite the early screening methods and hormone ablation therapies, prostate cancer (PCa) still remains the second leading cause of cancer-related mortality[1] in men in the western countries due to a higher incidence of metastasis[2]. PCa develops from a prostatic intraepithelial neoplasia (PIN) that eventually progresses towards invasive carcinoma[3]. The underlying mechanisms that determine the switch from normal to neoplastic and further to motile, invasive and metastatic cancer cells remain unclear.

Transforming growth factor β (TGFβ) isoforms[4] are among the best-characterized stimuli for phenotypic switching of a variety of cells such as myofibroblast differentiation[5–7], endothelial-to-mesenchymal transition (EndMT)[8] and epithelial-to-mesenchymal transition (EMT)[9]. Although a tumor suppressor early on[10, 11], prolonged stimulation by TGFβ induces EMT, shuns the tumor suppressive role, and promotes cancer invasion and metastasis[12, 13]. Although TGFβ1 induces apoptosis in prostate and bladder cancer cells via activation of P38 MAP kinase and JNK pathways[14], it induces PCa cell EMT via activation of Rac1 and P21 activated kinase-1 pathway[15, 16]. Thus, TGFβ1 is one of the first candidates known to engage in a dual, reciprocal role in the early and advanced cancers.

Akt (protein kinase B), a 3-gene family of serine-threonine kinase[17, 18] promotes oncogenic transformation[19] and tumor growth[20], including PCa[21–24]. Akt has also been implicated in the regulation of AR signaling to promote prostate tumor growth, where in $PTEN^{+/-}$ mice, AR was observed to be present both in the cytoplasm and the nucleus, in $PTEN^{+/-}/Akt1^{-/-}$ mice, AR was only localized in the nucleus [25]. However, the precise role of Akt in advanced cancer is not clear. We have reported that $Akt1^{-/-}$ mice exhibit increased vascular leakage and angiogenesis in response to vascular endothelial growth factor (VEGF) and melanoma xenografts[26]. Endothelial $Akt1^{-/-}$ mice exhibit vascular leakage via suppression of tight-junction claudins[27]. Similarly, overexpression of MyrAkt1 (active) in the prostate[28] and Akt activation in $PTEN^{-/-}$ mice[29, 30] although developed PIN, it did not progress to metastasis. Akt1 overexpression did not enhance breast cancer metastasis in $P53^{-/-}$ mice[31–33]. In a $TP53^{R270H}$ mouse model of prostate cancer, although the development of PIN was associated with increased Akt activation, invasive tumors indicated reduced Akt activation, suggesting that ‘Akt de-addiction’ may be necessary for attaining invasive ability[34]. Very recently, $Akt1^{-/-}/Akt2^{-/-}$ mice exhibited enhanced growth and metastasis in a drug-induced liver cancer model[35]. Thus, the increasing number of recent evidence suggests a context specific, the dual function of Akt in the early and advanced cancers.

In the current study, we compared the effects of early and late suppression of Akt on PCa growth and metastasis. In our study, $Akt1^{-/-}$ in TRansgenic Adenocarcinoma of the Mouse Prostate ($TRAMP/Akt1^{-/-}$) mice blunted oncogenic transformation, PIN, PCa and metastasis as compared to $TRAMP/Akt1^{+/+}$ mice. Interestingly, despite the delayed PIN and reduced PCa growth in heterozygous $TRAMP/Akt1^{+/-}$ mice, metastasis in these mice were similar to the $TRAMP/Akt1^{+/+}$ mice. Furthermore, pharmacological inhibition of Akt in advanced PCa bearing $TRAMP/Akt1^{+/+}$ mice or Akt1 gene silencing in aggressive human PCa cell lines promoted EMT and lung metastasis via decreased expression of β-catenin and

activation of the TGFβ1 pathway. Our study identifies Akt1-β-catenin signaling as a novel mechanism with dual, reciprocal role in the early and advanced PCa.

2. Materials and Methods

2.1. Generation and genotyping of TRAMP/Akt1$^{+/-}$ and TRAMP/Akt1$^{-/-}$ Mice

Akt1$^{-/-}$mice (C57BL/6 background) were generated and maintained as reported previously[26]. In order to generate *TRAMP/Akt1*$^{-/-}$ transgenic mice, C57BL/6 *Akt1*$^{+/-}$ male was crossed with *TRAMP* (C57BL/6 background) female mice (Jackson, Bar Harbor, ME). All experiments were carried out in accordance with guidelines set by VA Medical Center in Augusta. DNA was extracted from the tails of 10- to 21-day old litters (Qiagen, Valencia, CA). *TRAMP* transgene (600bp) was detected by PCR (forward: 5′-GCGCTGCTGACTTTCTAAACATAAG-3′ and reverse: 5′-GAGCTCACGTTAAGTTTTGATGTGT-3′) with an annealing temperature of 55°C. The internal positive control (forward: 5′-CTAGGCCACAGAATTGAAAGATCT-3′ and reverse: 5′-GTAGGTGGAAATTCAGCATCATCC-3′) produced a 324bp fragment. Primers to confirm Akt1 gene knockout (forward: 5′-TCCAGGACCAGGGGAGGATGTTTCTACTG-3′ and reverse: 5′-ACGACATGGTGCAGCAATGGCCAGCG-3′) yielded a 600bp band. Primers for *Neo* gene (forward: 5′-TGAGACGTGCTACTTCCATTTGTCACGTCC-3′ and reverse: 5′-ACAGGCCGCTACTATGCCATGAAGATCCTC-3′) generated a 1200bp fragment (Supplemental Figure 1).

2.2. Cell lines, reagents, and antibodies

Human PC3 and DU145 cells were obtained from ATCC (Manassas, VA). Cells were maintained in DMEM high glucose medium (Hyclone, Logan, UT) with 10% FBS (Atlanta Biologicals, GA), 100 U/ml penicillin, and 100 μg/ml streptomycin in a humidified incubator at 37°C and 5% CO_2, and routinely passaged when 80–90% confluent. Antibodies for pβ-catenin, β-catenin, E-cadherin, and N-cadherin were purchased from Cell Signaling (Danvers, MA). Anti-TGFβ-RII was purchased from Abcam (Cambridge, MA). Anti-β-actin was purchased from Sigma (St. Louis, MO). Compound inhibitors such as TCBN, ICG001, IWR-1, LY2109761, SB431542 and SB415286 were purchased from Selleckchem (Houston, TX).

2.3. ShRNA-mediated gene silencing and generation of stably silenced PCa cells

Human PC3 and DU145 cells were transfected with SMARTvector 2.0 Lentivirus ShAkt1 or non-targeting ShControl particles (GE Dharmacon, Lafayette, CO). Lentiviral infections were performed in 6 well plates. Lentiviral particles were mixed with 1ml SFM4 Transfx-293 (GE Hyclone, Lafayette, CO) solution and applied to PC3 and DU145 cells with 10 μg polybrene (American bioanalytical, MA). After 16 hours, the medium was replaced with complete EBM-2. After 3 days, GFP was detected using confocal imaging microscope (LSM510, Carl Zeiss, Germany). Stable silencing of Akt1 as compared to ShControl cells was achieved by puromycin selection (8 μg/ml, Thermo, Grand Island, NY). Post selection, cells were maintained in complete DMEM high glucose medium with 0.6 μg/ml puromycin.

2.4. Immunohistochemistry and staining of tissue sections

Mice were perfused with 4% paraformaldehyde in PBS prior to tissue collection. Prostate, kidney, lung and liver tissues were post-fixed and embedded either in paraffin or frozen blocks. Tissues were sliced (10 μm) for immunohistochemistry, H&E and Ki67 staining (Abcam, Cambridge, MA) followed by DAB staining (Thermo, Grand Island, NY). For immunostaining, frozen sections were washed with PBS, followed by incubation with 1% triton X-100 for 15min for permeabilization. Sections were blocked in 5% BSA in TBS for 30min followed by incubation with primary antibodies (Abcam, 1: 100 dilutions) overnight. Slides were washed with chilled PBS and incubated for another hour with Alexa Flour secondary antibodies at room temperature (Thermo, Grand Island, NY). After washing slides were mounted with Vectashield containing DAPI (Vector Laboratories, Burlingame, CA). Slides were viewed under the confocal imaging microscope (LSM510, Carl Zeiss, Germany).

2.5. Western blot analysis

Western blotting was performed as described previously[27] and protein concentration was determined by a Bradford protein assay kit (Bio-Rad, Hercules, USA). Samples were separated on 8–12 % SDS-PAGE gels, and then transferred onto PVDF membrane. Blotted membranes were blocked with 5 % milk or BSA for 30 minutes, followed by incubation with primary antibodies (1:1000 dilution) and with HRP-conjugated secondary antibodies (1: 5000, Abcam, Cambridge, MA). The proteins were visualized with ECL reagent (Thermo, Grand Island, NY).

2.6. qReal-Time PCR arrays

Twenty five-week-old *TRAMP/Akt1*$^{-/-}$ and *TRAMP/Akt1*$^{+/+}$ mice were treated with 10 mg/kg TCBN for 6 weeks, prostates were collected at 31 weeks and subjected to quantitative Real-Time PCR arrays. Briefly, tissues were lysed and RNA was isolated using RNeasy Mini Plus Kit (Qiagen, Valencia, CA) according to the manufacturer's protocol. Next cDNA was generated using RT2 First Strand Kit (SA Biosciences, Frederick, MD), mixed with qPCR SyberGreen master mix and loaded into Mouse PCa RT2 Profiler PCR Array plate (SA Biosciences, Frederick, MD). Reading was performed in Eppendorf Mastercycler realplex-2 equipment (Eppendorf, Hauppauge, NY).

2.7. Terminal deoxynucleotidyl transferase-mediated dUTP nick end labeling (TUNEL) assay

The TUNEL assay for the *in situ* detection of apoptosis in frozen sections was performed using the ApopTag® green *In Situ* apoptosis detection kit (Millipore, Billerica, MA) as described before[27].

2.8. Mouse model of experimental lung metastasis

Ten-week-old athymic nude mice (Harlan, Indianapolis, IN) were divided into two groups for the administration of PC3 cells expressing control and Akt1 ShRNA. Cells (0.5×10^6) suspended in sterile normal saline were administered (*i.v.*) to each group of mice separately via the tail vein. In all the experiments, mice were evaluated for the presence of metastases 3

days and 2 weeks after PC3 cell administration. PC3 cell metastasis to the lungs cells was detected using IRDye 800CW 2-DG optical probe injected to the mice (*i.v.*) 24 hours prior to imaging. This fluorescent reagent has been shown to be up-taken predominantly by the tumor cells *in vivo*[36]. The signals of IRDye 800CW 2-DG were collected by Pearl impulse imaging system (LiCOR Inc. Lincoln, NE) 24 hours after injection. To avoid a high background noise in the signal, we performed imaging of the organs directly. In addition to the imaging, analysis of lung, liver and kidney metastasis was performed using immunohistochemistry and fluorescence imaging.

2.9. Statistical Analysis

All the data are presented as mean ± SD and were calculated from multiple independent experiments performed in quadruplicates. For normalized data analysis, data was confirmed that normality assumption was satisfied and analyzed using paired sample t-test (dependent t-test) and/or further confirmed with non-parametric test Wilcoxon signed rank test. For all other analyses, Student's two-tailed t-test or ANOVA test were used to determine significant differences between treatment and control values using the GraphPad Prism 4.03 software and SPSS 17.0 software. Data with $P<0.05$ were considered significant.

3. Results

3.1. Akt1 deficiency abrogates oncogenic transformation in TRAMP mouse prostate

TRAMP is an autochthonous mouse model that develops PCa in defined stages during growth that mimics the initiation of human disease and any hormonal or chemical treatment[37, 38]. *TRAMP* develop PIN at 12 weeks, PCa at 24 weeks, and metastasis to the lung and liver at 31 weeks of age[37, 39]. In our study, we found the same pattern with tumor sizes smaller in *TRAMP/Akt1*$^{+/-}$ mice as compared to *TRAMP/Akt1*$^{+/+}$ mice. Interestingly, neither PIN nor tumors were developed in the *TRAMP/Akt1*$^{-/-}$ mice even until 31 weeks (Figure 1A–B and Supplemental Figure 2). Whereas *TRAMP/Akt1*$^{+/+}$ mice developed prostate tumors by 24 weeks, prostate weight was significantly lesser in *TRAMP/Akt1*$^{+/-}$ mice, and no tumors developed in *TRAMP/Akt1*$^{-/-}$ mice at 24 and 31 weeks (Figure 1C). Overall, Akt1 gene ablation prevented oncogenic transformation and tumor development in *TRAMP* mice.

3.2. Akt1 loss in TRAMP prostate promotes apoptosis, suppresses proliferation, and increases lifespan

Since Akt promotes cell survival[18], we assumed *TRAMP/Akt1*$^{-/-}$prostates will have increased apoptosis. *TRAMP/Akt1*$^{+/+}$, *TRAMP/Akt1*$^{+/-}$ and *TRAMP/Akt1*$^{-/-}$prostates were collected at 12 (PIN stage) and 31 weeks (advanced tumor stage) and the sections were subjected to TUNEL and Ki67 staining. At both 12 and 31 weeks, TUNEL positive cells were significantly higher and Ki67 positive cells were significantly lower in *TRAMP/Akt1*$^{-/-}$prostates compared to *TRAMP/Akt1*$^{+/+}$ and *TRAMP/Akt1*$^{+/-}$ prostates (Figure 2A–C). A significant increase in the levels of pro-apoptotic cleaved caspase-3 and cleaved p18 and p43/48 caspase-8 in *TRAMP/Akt1*$^{-/-}$prostates compared to *TRAMP/Akt1*$^{+/+}$ and *TRAMP/Akt1*$^{+/-}$ prostates were observed (Figure 2D–E).

3.3. Late suppression of Akt activity in advanced PCa in TRAMP mice promotes metastasis

A Kaplan-Meier plot based on a 400 day follow up on these mice showed no loss of life in any *TRAMP/Akt1*$^{-/-}$ mice during this period (Figure 3A). All of the *TRAMP/Akt1*$^{+/+}$ mice died between days 200 and 350 (28–50 weeks), a period of advanced PCa growth and metastasis in *TRAMP* mice. Surprisingly, median survival time was 216 days for *TRAMP/Akt1*$^{+/+}$ mice and 228 days for *TRAMP/Akt1*$^{+/-}$ mice indicating that partial loss of Akt1 does not improve the life expectancy (Figure 3A). Our analysis of serial sections of mouse prostate revealed that almost all of the *TRAMP/Akt1*$^{+/+}$ and *TRAMP/Akt1*$^{+/-}$ mice developed metastasis to the lungs, liver, and kidneys (Figure 3B). In contrast, none of the *TRAMP/Akt1*$^{-/-}$ mice showed signs of metastasis in any of the tissues (Figure 3B), indicating that partial Akt1 suppression promotes PCa metastasis in *TRAMP* mice, despite delayed PIN and tumor growth.

In order to determine the role of Akt in the advanced stages of PCa, we treated 25-week old *TRAMP* mice with Akt inhibitor TCBN for 6 weeks. At 31 weeks, prostate, lungs, liver, and kidneys were collected from 6-week TCBN treated *TRAMP* mice, and were subjected to immunohistochemistry. Our analysis showed that 6-week treatment with TCBN only had a modest effect on tumor growth as compared to the dramatic effect of Akt1 suppression during the early stages of prostate tumor growth in *TRAMP* mice (Figure 3C). Surprisingly, TCBN treated *TRAMP* mice exhibited enhanced metastasis of PCa cells into the liver and lungs compared to DMSO treated control mice (Figure 3D–F). A 4-fold increase in the number of metastatic colonies was found in TCBN-treated mouse lungs compared to DMSO-treated controls, thus demonstrating that late Akt suppression during the advanced stages of PCa promotes metastasis to the lungs and liver.

3.4. Silencing of Akt1 gene expression in human PCa (PC3) cells promotes metastasis to the lungs

To determine the clinical relevance of our results from the *TRAMP* mice on the role of Akt in PCa metastasis, we sought to confirm our findings in human PCa cell line. In order to do that, we generated control (ShControl) and Akt1 deficient (ShAkt1) PC3 cell lines using ShRNA-mediated stable silencing of Akt1 through lentiviral infection, followed by antibiotic selection. Athymic nude mice intravenously administered with ShAkt1 PC3 cells exhibited increased presence of metastasized PCa colonies in the lungs and liver on day 3 after administration, as compared to the mice administered with ShControl PC3 cells (Figure 4A–C). Interestingly, 2 weeks after the administration of ShAkt1 PC3 cells in athymic nude mice, we observed an 8-fold increase in the presence of metastasized PCa colonies in the lungs compared to ShControl PC3 cells (Figure 4D–E). Such a difference, however, was not observed in liver metastasis (Figure 4E).

Analysis of lung tissues 3 days after the administration of PCa cells indicated that mice administered with ShAkt1 PC3 cells had a higher number of PCa cells in the lungs compared to the mice administered with ShControl PC3 cells (Figure 5A, B, and F). This difference was even higher in lungs collected 2 weeks after administration (Figure 5C, D, and F), with ShAkt1 PC3 cells showing 40% higher rate of metastasis compared to ShControl cell administered mice (Figure 5H). However, a significant difference between

ShControl and ShAkt1 PC3 cells on liver metastasis was not observed (Figure 5E–H). Altogether, these results convincingly demonstrate that Akt suppression or Akt1 gene ablation in advanced PCa promotes metastasis.

3.5. Akt inhibition in TRAMP mice and Akt1 loss in human PCa cells promote EMT

When EMT is initiated in cancer, loss of polarity and altered communication with the extracellular matrix (ECM) result in invasion and metastasis [40]. In order to determine whether EMT has contributed to enhanced metastasis with Akt suppression in advanced PCa, we examined changes in the expression of epithelial and mesenchymal markers. Our qPCR gene array analysis of *TRAMP* prostate treated with DMSO and TCBN indicated a significant increase in EMT markers such as Goosecoid homeobox, matrix metalloproteases-3 and -9 (MMP3/9), Snail1, SOX-10, BMP7, Nodal, GSK3β, and N-cadherin etc. (Figure 6A; Supplemental Figure 3). Further, Western blot analysis of prostate tissues confirmed an increase in the expression of mesenchymal markers N-cadherin and Snail1 associated with a decrease in the expression of epithelial marker E-cadherin in TCBN treated *TRAMP* prostate compared to DMSO treated control prostate (Figure 6B–C). Similarly, Akt1 gene silencing in PC3 and DU145 cells resulted in significant increase in the expression of mesenchymal marker N-cadherin (Figure 6D–F). Although the expression of epithelial marker E-cadherin was below detectable levels in ShControl and ShAkt1 PC3 cells, we observed a dramatic decrease, almost a total loss of E-cadherin expression in ShAkt1 DU145 cells compared to ShControl DU145 cells (Figure 6D–F), indicating promotion of EMT upon suppression of Akt(1) activity in advanced PCa cells.

3.6. PCa cell EMT as result of Akt1 suppression is dependent on the activation of TGFβ1signaling and transcriptional suppression of β-catenin

Since TGFβ is a major promoter of EMT in many cancer cells, we wanted to determine the changes in the activation of TGFβ pathway with Akt1 gene silencing. Western blot analysis of ShControl and ShAkt1 PC3 and DU145 cells revealed increased expression of TGFβ1 and its receptor TGFβ-RII in ShAkt1 PC3 and DU145 cells as compared to their respective ShControl cells (Figure 7A–B). Since we observed a near to total loss of E-cadherin in ShAkt1 DU145 cells, we next determined if inhibition of TGFβ pathway could reverse the E-cadherin loss in ShAkt1 DU145 cells. Intriguingly, treatment with TGFβ-R inhibitors LY2109761 and SB431542 reversed the loss of E-cadherin in ShAkt1 DU145 cells (Figure 7C–D), thus indicating that TGFβ1-mediated pathway is activated in PCa cells upon Akt1 gene silencing.

In order to further determine the candidate downstream of Akt1 loss that is responsible for the activation of the TGFβ1 pathway in PCa cells, we looked at the activity status of GSK-3/β-catenin signaling. Our analysis suggested that, in addition to Akt1 and TGFβ, β-catenin may also be playing a dual role during the early and later stages of PCa progression. Our initial analysis indicated a decrease in the expression of phosphorylated and total β-catenin levels in ShAkt1 PC3 and DU145 cells compared to their respective ShControl cells (Figure 8A–B). Interestingly, loss of phosphorylated β-catenin was modestly but significantly reversed upon treatment with β-catenin transcription inhibitor ICG001 (Figure 8C–D). Similarly, treatment with β-catenin transcription inhibitors ICG001 and IWR-1 also resulted

in increased expression of mesenchymal marker N-cadherin in both PC3 and DU145 cells (Figure 8E–F). Furthermore, our results indicated a significant increase in N-cadherin expression in DU145 cells upon treatment with TGFβ1, which was reversible upon co-treatment with TGFβ-R inhibitors (Figure 8G–H). Interestingly, treatment of DU145 cells with ICG001 resulted in increased N-cadherin expression comparable to the level of TGFβ1-induced N-cadherin expression (Figure 8G–H), thus indicating that suppression of β-catenin transcriptional activity downstream of Akt1 inhibition leads to EMT and promotion of metastasis in advanced PCa cells.

4. Discussion

Epithelial cells, in their normal state, enable characteristic cobblestone shape, basolateral cell polarity and cell-cell contacts via their adherens- and tight-junctions[41]. These cell-junctions are kept intact and the contact-dependent inhibition of proliferation is assured through the expression of several specific markers such as E-cadherin, β-catenin, claudins etc[42]. Tumor suppressor proteins such as p53 help to maintain epithelial cell polarity through the protection of epithelial-barrier[43]. Cellular mutations disrupt epithelial-barrier and compromise the basolateral cell polarity, thus promoting asymmetric cell division and oncogenic transformation leading to tumor initiation and growth[44]. These initiated tumor cells further undergo cellular transformations to attain invasive phenotype by shedding epithelial markers such as E-cadherins and keratins, and by gaining *de novo* mesenchymal markers such as N-cadherin, vimentin, snail1 etc[35]. This process known as EMT imparts the initiated cancer cells a spindle-shaped, motile and invasive mesenchymal phenotype that are a pre-requisite for cancer metastasis.

The mechanisms regulating EMT in cancer are not well characterized. While most early stage tumor cells maintain some epithelial characteristics, a few develop quasi-mesenchymal features expressing both epithelial and mesenchymal markers[35]. A total switch to mesenchymal phenotype is not achieved even when these cancer cells have attained aggressive features[45]. Thus, epithelial tumors consist of a heterogeneous population of cancer cells with the multifarious potential to proliferate, migrate, invade and metastasize[46]. This heterogeneity occurs due to the constant evolution of cancer cells to resist and survive in an offensive tumor microenvironment, where the same stromal cells that fight to limit early tumor expansion are modified by the cancer cells to their benefit in advanced stages[47, 48]. The step-wise phenotypic switching of early tumor cells to more aggressive ones is ensured by various tumor-derived growth factors, changes in the expression of cell surface proteins, and activity modulation of several intracellular signaling pathways[46, 49, 50].

In addition to the basic cellular functions of Akt, an important aspect that we, as the Akt-centric researchers have noticed is its dual nature during the early and late stages of pathologies. Whereas Akt promotes VEGF-induced endothelial cell activation, $Akt1^{-/-}$endothelial cells exhibit enhanced vascular permeability[18, 26]. Although $Akt1^{-/-}$ cardiomyocytes exhibit apoptosis following ischemia, Akt1 loss in the later stages improves function[51] by inhibiting fibrosis[5, 52, 53] and oxidative stress[54]. In cancer, although Akt promotes PCa[21–24, 55], whether or not Akt is a determinant factor in making the

switch from early to aggressive PCa is not known. Interestingly, recent studies in various cancers suggest otherwise. First *in vitro* evidence on reduced invasive migration of breast cancer cells with Akt1 suppression came from Alex Toker's laboratory[56, 57]. Akt1 inhibition also promoted tuberous sclerosis complex-2 (TSC-2) activation leading to breast cancer invasion *in vitro*[58] and was predictive of decreased time to metastasize in patients. Following this, Tsichlis laboratory reported that Akt1 knockdown in aggressive breast cancer cells results in reduced miRNA200 expression promoting EMT[59] and active Akt1 overexpression did not enhance breast cancer metastasis in $P53^{-/-}$ mice[31–33]. The only report on the effect of Akt1/Akt2 knockout in augmenting drug-induced liver cancer *in vivo* came very recently from Nissim Hay's laboratory[35]. Despite these controversial reports, TCBN, an Akt inhibitor[60, 61] is currently in phase III clinical trials.

Similar to $PTEN/Akt1^{-/-}$ mice[25], we observed no occurrence of PCa metastasis in $TRAMP/Akt1^{-/-}$ mice. However, these models pose a serious question that when $PTEN/Akt1^{-/-}$and $TRAMP/Akt1^{-/-}$ mice do not develop prostate tumors, how is the incidence of metastasis even possible? As in the case of PCa patients, where treatment is not possible until a tumor is detected, a clinically relevant model to test the efficacy of targeting a molecule for advanced PCa is the one that allows treatment once after the tumor is developed. Thus, our results from 31-week old prostate tumor bearing *TRAMP* mice treated with triciribine indicated that targeting Akt in advanced PCa can worsen the outcome by promoting EMT and enhancing metastasis.

We demonstrated that GSK-3α and GSK-3β elicit isoform-specific effects on PCa cells, and that GSK-3β is directly involved in the regulation of PCa cell invasion involving internalization of β-catenin[62]. Isoform-specific GSK-3 localization is also reported in early vs advanced PCa patient samples[63]. Similar to TGFβ and Akt, reports on the role of β-catenin in advanced cancers have also been conflicting[64, 65]. Whereas β-catenin promotes early PCa growth via associating with androgen receptor signaling[66], advanced PCa tissues with a history of metastasis have indicated lower nuclear β-catenin[67]. The decrease in E-cadherin and α-β-γ-catenins has also been reported in breast[68] and PCa metastasis[69]. Interestingly, agents such as mirtazapine that effectively limit human cancer metastasis correlated with increased β-catenin levels[70]. In contrast, there are also studies indicating metastasis-promoting effects of β-catenin activation[71, 72]. While these discrepancies may be due to the existence of two different pools of β-catenin in PCa cells in the barrier-junctions and Wnt complex[65], our results on the effect of TGFβ-R inhibitors and compounds that directly block the nuclear localization of β-catenin demonstrate that suppression of β-catenin expression and elevated levels of active TGFβ1 in $Akt1^{-/-}$ PCa cells promote EMT and metastasis.

In conclusion, we report for the first time that although Akt1 is essential for the oncogenic transformation and PCa growth, Akt1 suppression in advanced PCa promotes EMT and metastasis *in vivo*, via increased expression of Snail1, Sox-10, Goosecoid and N-cadherin, activation of TGFβ1, and suppression of E-cadherin and β-catenin expressions. Although targeting TGFβ pathway is a viable option for the treatment of metastatic PCa, our study points out the need for further confirmation of Akt1 inhibitors such as triciribine and β-catenin inhibitors such as ICG001 for utilizing in the treatment of metastatic PCa.

Supplementary Material

Refer to Web version on PubMed Central for supplementary material.

Acknowledgments

Funds were provided by the National Institutes of Health grant (R01HL103952) and in part by the Wislon Pharmacy Foundation to PRS. Funding from The National Natural Science Foundation of China to FG (81672893) is acknowledged. This work has been accomplished using the resources and facilities at the VA Medical Center in Augusta, GA. The funders had no role in the study design, data collection, analysis, and decision to publish the data. The contents of the manuscript do not represent the views of Department of Veteran Affairs or the United States Government.

References

1. Siegel RL, Miller KD, Jemal A. Cancer statistics, 2016. CA: a cancer journal for clinicians. 2016; 66:7–30. [PubMed: 26742998]
2. Crawford ED, Higano CS, Shore ND, Hussain M, Petrylak DP. Treating Patients with Metastatic Castration Resistant Prostate Cancer: A Comprehensive Review of Available Therapies. The Journal of urology. 2015; 194:1537–1547. [PubMed: 26196735]
3. Schoenfield L, Jones JS, Zippe CD, Reuther AM, Klein E, Zhou M, Magi-Galluzzi C. The incidence of high-grade prostatic intraepithelial neoplasia and atypical glands suspicious for carcinoma on first-time saturation needle biopsy, and the subsequent risk of cancer. BJU international. 2007; 99:770–774. [PubMed: 17233800]
4. Wakefield LM, Hill CS. Beyond TGFbeta: roles of other TGFbeta superfamily members in cancer. Nature reviews Cancer. 2013; 13:328–341. [PubMed: 23612460]
5. Abdalla M, Sabbineni H, Prakash R, Ergul A, Fagan SC, Somanath PR. The Akt inhibitor, triciribine, ameliorates chronic hypoxia-induced vascular pruning and TGFbeta-induced pulmonary fibrosis. British journal of pharmacology. 2015; 172:4173–4188. [PubMed: 26033700]
6. Stempien-Otero A, Kim DH, Davis J. Molecular networks underlying myofibroblast fate and fibrosis. Journal of molecular and cellular cardiology. 2016; 97:153–161. [PubMed: 27167848]
7. Fan Z, Guan J. Antifibrotic therapies to control cardiac fibrosis. Biomaterials research. 2016; 20:13. [PubMed: 27226899]
8. Gonzalez DM, Medici D. Signaling mechanisms of the epithelial-mesenchymal transition. Science signaling. 2014; 7:re8. [PubMed: 25249658]
9. Zhang J, Tian XJ, Xing J. Signal Transduction Pathways of EMT Induced by TGF-beta, SHH, and WNT and Their Crosstalks. Journal of clinical medicine. 2016; 5
10. Serra R, Moses HL. Tumor suppressor genes in the TGF-beta signaling pathway? Nature medicine. 1996; 2:390–391.
11. Siegel PM, Massague J. Cytostatic and apoptotic actions of TGF-beta in homeostasis and cancer. Nature reviews Cancer. 2003; 3:807–821. [PubMed: 14557817]
12. Chen W, Zhou S, Mao L, Zhang H, Sun D, Zhang J, Li J, Tang JH. Crosstalk between TGF-beta signaling and miRNAs in breast cancer metastasis. Tumour biology: the journal of the International Society for Oncodevelopmental Biology and Medicine. 2016
13. Massague J. How cells read TGF-beta signals. Nature reviews Molecular cell biology. 2000; 1:169–178. [PubMed: 11252892]
14. Al-Azayzih A, Gao F, Goc A, Somanath PR. TGFbeta1 induces apoptosis in invasive prostate cancer and bladder cancer cells via Akt-independent, p38 MAPK and JNK/SAPK-mediated activation of caspases. Biochemical and biophysical research communications. 2012; 427:165–170. [PubMed: 22989755]
15. Goc A, Al-Azayzih A, Abdalla M, Al-Husein B, Kavuri S, Lee J, Moses K, Somanath PR. P21 activated kinase-1 (Pak1) promotes prostate tumor growth and microinvasion via inhibition of transforming growth factor beta expression and enhanced matrix metalloproteinase 9 secretion. The Journal of biological chemistry. 2013; 288:3025–3035. [PubMed: 23258534]

16. Al-Azayzih A, Gao F, Somanath PR. P21 activated kinase-1 mediates transforming growth factor beta1-induced prostate cancer cell epithelial to mesenchymal transition. Biochimica et biophysica acta. 2015; 1853:1229–1239. [PubMed: 25746720]
17. Blume-Jensen P, Hunter T. Oncogenic kinase signalling. Nature. 2001; 411:355–365. [PubMed: 11357143]
18. Somanath PR, Razorenova OV, Chen J, Byzova TV. Akt1 in endothelial cell and angiogenesis. Cell cycle. 2006; 5:512–518. [PubMed: 16552185]
19. Somanath PR, Vijai J, Kichina JV, Byzova T, Kandel ES. The role of PAK-1 in activation of MAP kinase cascade and oncogenic transformation by Akt. Oncogene. 2009; 28:2365–2369. [PubMed: 19421139]
20. Brugge J, Hung MC, Mills GB. A new mutational AKTivation in the PI3K pathway. Cancer cell. 2007; 12:104–107. [PubMed: 17692802]
21. Kochuparambil ST, Al-Husein B, Goc A, Soliman S, Somanath PR. Anticancer efficacy of simvastatin on prostate cancer cells and tumor xenografts is associated with inhibition of Akt and reduced prostate-specific antigen expression. The Journal of pharmacology and experimental therapeutics. 2011; 336:496–505. [PubMed: 21059805]
22. Goc A, Al-Husein B, Kochuparambil ST, Liu J, Heston WW, Somanath PR. PI3 kinase integrates Akt and MAP kinase signaling pathways in the regulation of prostate cancer. International journal of oncology. 2011; 38:267–277. [PubMed: 21109949]
23. Goc A, Liu J, Byzova TV, Somanath PR. Akt1 mediates prostate cancer cell microinvasion and chemotaxis to metastatic stimuli via integrin beta(3) affinity modulation. British journal of cancer. 2012; 107:713–723. [PubMed: 22767145]
24. Goc A, Kochuparambil ST, Al-Husein B, Al-Azayzih A, Mohammad S, Somanath PR. Simultaneous modulation of the intrinsic and extrinsic pathways by simvastatin in mediating prostate cancer cell apoptosis. BMC cancer. 2012; 12:409. [PubMed: 22974127]
25. Chen ML, Xu PZ, Peng XD, Chen WS, Guzman G, Yang X, Di Cristofano A, Pandolfi PP, Hay N. The deficiency of Akt1 is sufficient to suppress tumor development in Pten+/− mice. Genes & development. 2006; 20:1569–1574. [PubMed: 16778075]
26. Chen J, Somanath PR, Razorenova O, Chen WS, Hay N, Bornstein P, Byzova TV. Akt1 regulates pathological angiogenesis, vascular maturation and permeability in vivo. Nature medicine. 2005; 11:1188–1196.
27. Gao F, Artham S, Sabbineni H, Al-Azayzih A, Peng XD, Hay N, Adams RH, Byzova TV, Somanath PR. Akt1 promotes stimuli-induced endothelial-barrier protection through FoxO-mediated tight-junction protein turnover. Cellular and molecular life sciences: CMLS. 2016
28. Majumder PK, Yeh JJ, George DJ, Febbo PG, Kum J, Xue Q, Bikoff R, Ma H, Kantoff PW, Golub TR, Loda M, Sellers WR. Prostate intraepithelial neoplasia induced by prostate restricted Akt activation: the MPAKT model. Proceedings of the National Academy of Sciences of the United States of America. 2003; 100:7841–7846. [PubMed: 12799464]
29. Blanco-Aparicio C, Renner O, Leal JF, Carnero A. PTEN, more than the AKT pathway. Carcinogenesis. 2007; 28:1379–1386. [PubMed: 17341655]
30. Li B, Sun A, Youn H, Hong Y, Terranova PF, Thrasher JB, Xu P, Spencer D. Conditional Akt activation promotes androgen-independent progression of prostate cancer. Carcinogenesis. 2007; 28:572–583. [PubMed: 17032658]
31. Hutchinson J, Jin J, Cardiff RD, Woodgett JR, Muller WJ. Activation of Akt (protein kinase B) in mammary epithelium provides a critical cell survival signal required for tumor progression. Molecular and cellular biology. 2001; 21:2203–2212. [PubMed: 11238953]
32. Hutchinson JN, Jin J, Cardiff RD, Woodgett JR, Muller WJ. Activation of Akt-1 (PKB-alpha) can accelerate ErbB-2-mediated mammary tumorigenesis but suppresses tumor invasion. Cancer research. 2004; 64:3171–3178. [PubMed: 15126356]
33. Ackler S, Ahmad S, Tobias C, Johnson MD, Glazer RI. Delayed mammary gland involution in MMTV-AKT1 transgenic mice. Oncogene. 2002; 21:198–206. [PubMed: 11803463]
34. Vinall RL, Chen JQ, Hubbard NE, Sulaimon SS, Shen MM, Devere White RW, Borowsky AD. Initiation of prostate cancer in mice by Tp53R270H: evidence for an alternative molecular progression. Disease models & mechanisms. 2012; 5:914–920. [PubMed: 22563073]

35. Wang Q, Yu WN, Chen X, Peng XD, Jeon SM, Birnbaum MJ, Guzman G, Hay N. Spontaneous Hepatocellular Carcinoma after the Combined Deletion of Akt Isoforms. Cancer cell. 2016; 29:523–535. [PubMed: 26996309]
36. Kovar JL, Volcheck W, Sevick-Muraca E, Simpson MA, Olive DM. Characterization and performance of a near-infrared 2-deoxyglucose optical imaging agent for mouse cancer models. Analytical biochemistry. 2009; 384:254–262. [PubMed: 18938129]
37. Gingrich JR, Barrios RJ, Foster BA, Greenberg NM. Pathologic progression of autochthonous prostate cancer in the TRAMP model. Prostate cancer and prostatic diseases. 1999; 2:70–75. [PubMed: 12496841]
38. Greenberg NM, DeMayo F, Finegold MJ, Medina D, Tilley WD, Aspinall JO, Cunha GR, Donjacour AA, Matusik RJ, Rosen JM. Prostate cancer in a transgenic mouse. Proceedings of the National Academy of Sciences of the United States of America. 1995; 92:3439–3443. [PubMed: 7724580]
39. Howe SR, Pass HI, Ethier SP, Matthews WJ, Walker C. Presence of an insulin-like growth factor I autocrine loop predicts uterine fibroid responsiveness to tamoxifen. Cancer research. 1996; 56:4049–4055. [PubMed: 8752178]
40. Lee JM, Dedhar S, Kalluri R, Thompson EW. The epithelial-mesenchymal transition: new insights in signaling, development, and disease. The Journal of cell biology. 2006; 172:973–981. [PubMed: 16567498]
41. Yu Y, Elble RC. Homeostatic Signaling by Cell-Cell Junctions and Its Dysregulation during Cancer Progression. Journal of clinical medicine. 2016; 5
42. Royer C, Lu X. Epithelial cell polarity: a major gatekeeper against cancer? Cell death and differentiation. 2011; 18:1470–1477. [PubMed: 21617693]
43. Roger L, Gadea G, Roux P. Control of cell migration: a tumour suppressor function for p53? Biology of the cell/under the auspices of the European Cell Biology Organization. 2006; 98:141–152.
44. Ashaie MA, Chowdhury EH. Cadherins: The Superfamily Critically Involved in Breast Cancer. Current pharmaceutical design. 2016; 22:616–638. [PubMed: 26825466]
45. Fischer KR, Durrans A, Lee S, Sheng J, Li F, Wong ST, Choi H, El Rayes T, Ryu S, Troeger J, Schwabe RF, Vahdat LT, Altorki NK, Mittal V, Gao D. Epithelial-to-mesenchymal transition is not required for lung metastasis but contributes to chemoresistance. Nature. 2015; 527:472–476. [PubMed: 26560033]
46. Heerboth S, Housman G, Leary M, Longacre M, Byler S, Lapinska K, Willbanks A, Sarkar S. EMT and tumor metastasis. Clinical and translational medicine. 2015; 4:6. [PubMed: 25852822]
47. Criscitiello C, Esposito A, Curigliano G. Tumor-stroma crosstalk: targeting stroma in breast cancer. Current opinion in oncology. 2014; 26:551–555. [PubMed: 25279962]
48. Klemm F, Joyce JA. Microenvironmental regulation of therapeutic response in cancer. Trends in cell biology. 2015; 25:198–213. [PubMed: 25540894]
49. Guan X. Cancer metastases: challenges and opportunities. Acta pharmaceutica Sinica B. 2015; 5:402–418. [PubMed: 26579471]
50. Hunter KW, Crawford NP, Alsarraj J. Mechanisms of metastasis. Breast cancer research: BCR. 2008; 10(Suppl 1):S2.
51. Ma L, Kerr BA, Naga Prasad SV, Byzova TV, Somanath PR. Differential effects of Akt1 signaling on short- versus long-term consequences of myocardial infarction and reperfusion injury. Laboratory investigation; a journal of technical methods and pathology. 2014; 94:1083–1091. [PubMed: 25046438]
52. Somanath PR, Kandel ES, Hay N, Byzova TV. Akt1 signaling regulates integrin activation, matrix recognition, and fibronectin assembly. The Journal of biological chemistry. 2007; 282:22964–22976. [PubMed: 17562714]
53. Abdalla M, Goc A, Segar L, Somanath PR. Akt1 mediates alpha-smooth muscle actin expression and myofibroblast differentiation via myocardin and serum response factor. The Journal of biological chemistry. 2013; 288:33483–33493. [PubMed: 24106278]
54. Kerr BA, Ma L, West XZ, Ding L, Malinin NL, Weber ME, Tischenko M, Goc A, Somanath PR, Penn MS, Podrez EA, Byzova TV. Interference with akt signaling protects against myocardial

infarction and death by limiting the consequences of oxidative stress. Science signaling. 2013; 6:ra67. [PubMed: 23921086]

55. Goc A, Al-Husein B, Katsanevas K, Steinbach A, Lou U, Sabbineni H, DeRemer DL, Somanath PR. Targeting Src-mediated Tyr216 phosphorylation and activation of GSK-3 in prostate cancer cells inhibit prostate cancer progression in vitro and in vivo. Oncotarget. 2014; 5:775–787. [PubMed: 24519956]
56. Yoeli-Lerner M, Chin YR, Hansen CK, Toker A. Akt/protein kinase b and glycogen synthase kinase-3beta signaling pathway regulates cell migration through the NFAT1 transcription factor. Molecular cancer research: MCR. 2009; 7:425–432. [PubMed: 19258413]
57. Toker A, Yoeli-Lerner M. Akt signaling and cancer: surviving but not moving on. Cancer research. 2006; 66:3963–3966. [PubMed: 16618711]
58. Liu H, Radisky DC, Nelson CM, Zhang H, Fata JE, Roth RA, Bissell MJ. Mechanism of Akt1 inhibition of breast cancer cell invasion reveals a protumorigenic role for TSC2. Proceedings of the National Academy of Sciences of the United States of America. 2006; 103:4134–4139. [PubMed: 16537497]
59. Iliopoulos D, Polytarchou C, Hatziapostolou M, Kottakis F, Maroulakou IG, Struhl K, Tsichlis PN. MicroRNAs differentially regulated by Akt isoforms control EMT and stem cell renewal in cancer cells. Science signaling. 2009; 2:ra62. [PubMed: 19825827]
60. Schilcher RB, Haas CD, Samson MK, Young JD, Baker LH. Phase I evaluation and clinical pharmacology of tricyclic nucleoside 5′-phosphate using a weekly intravenous regimen. Cancer research. 1986; 46:3147–3151. [PubMed: 3698029]
61. Hoffman K, Holmes FA, Fraschini G, Esparza L, Frye D, Raber MN, Newman RA, Hortobagyi GN. Phase I-II study: triciribine (tricyclic nucleoside phosphate) for metastatic breast cancer. Cancer chemotherapy and pharmacology. 1996; 37:254–258. [PubMed: 8529286]
62. Gao F, Al-Azayzih A, Somanath PR. Discrete functions of GSK3alpha and GSK3beta isoforms in prostate tumor growth and micrometastasis. Oncotarget. 2015; 6:5947–5962. [PubMed: 25714023]
63. Darrington RS, Campa VM, Walker MM, Bengoa-Vergniory N, Gorrono-Etxebarria I, Uysal-Onganer P, Kawano Y, Waxman J, Kypta RM. Distinct expression and activity of GSK-3alpha and GSK-3beta in prostate cancer. International journal of cancer. 2012; 131:E872–883. [PubMed: 22539113]
64. Wei W, Zeve D, Suh JM, Wang X, Du Y, Zerwekh JE, Dechow PC, Graff JM, Wan Y. Biphasic and dosage-dependent regulation of osteoclastogenesis by beta-catenin. Molecular and cellular biology. 2011; 31:4706–4719. [PubMed: 21876000]
65. Kypta RM, Waxman J. Wnt/beta-catenin signalling in prostate cancer. Nature reviews Urology. 2012; 9:418–428. [PubMed: 22710668]
66. Yardy GW, Brewster SF. Wnt signalling and prostate cancer. Prostate cancer and prostatic diseases. 2005; 8:119–126. [PubMed: 15809669]
67. Horvath LG, Henshall SM, Lee CS, Kench JG, Golovsky D, Brenner PC, O'Neill GF, Kooner R, Stricker PD, Grygiel JJ, Sutherland RL. Lower levels of nuclear beta-catenin predict for a poorer prognosis in localized prostate cancer. International journal of cancer. 2005; 113:415–422. [PubMed: 15455387]
68. Bukholm IK, Nesland JM, Karesen R, Jacobsen U, Borresen-Dale AL. E-cadherin and alpha-, beta-, and gamma-catenin protein expression in relation to metastasis in human breast carcinoma. The Journal of pathology. 1998; 185:262–266. [PubMed: 9771479]
69. Pontes J Jr, Srougi M, Borra PM, Dall' Oglio MF, Ribeiro-Filho LA, Leite KR. E-cadherin and beta-catenin loss of expression related to bone metastasis in prostate cancer. Applied immunohistochemistry & molecular morphology: AIMM/official publication of the Society for Applied Immunohistochemistry. 2010; 18:179–184.
70. Uzawa K, Kasamatsu A, Shimizu T, Saito Y, Baba T, Sakuma K, Fushimi K, Sakamoto Y, Ogawara K, Shiiba M, Tanzawa H. Suppression of metastasis by mirtazapine via restoration of the Lin-7C/beta-catenin pathway in human cancer cells. Scientific reports. 2014; 4:5433. [PubMed: 24961284]
71. Liu W, Xing F, Iiizumi-Gairani M, Okuda H, Watabe M, Pai SK, Pandey PR, Hirota S, Kobayashi A, Mo YY, Fukuda K, Li Y, Watabe K. N-myc downstream regulated gene 1 modulates Wnt-beta-

catenin signalling and pleiotropically suppresses metastasis. EMBO molecular medicine. 2012; 4:93–108. [PubMed: 22246988]

72. Francis JC, Thomsen MK, Taketo MM, Swain A. beta-catenin is required for prostate development and cooperates with Pten loss to drive invasive carcinoma. PLoS genetics. 2013; 9:e1003180. [PubMed: 23300485]

HIGHLIGHTS

- Akt1 deficiency blunts oncogenic transformation and prostate cancer growth
- Akt1 inhibition in advanced prostate cancer promote metastasis
- Akt1 loss in advanced prostate cancer promote epithelial-to-mesenchymal transition
- Akt1 suppression in advanced prostate cancer suppress β-catenin expression
- β-catenin inhibition in PC3 and DU145 cells promote mesenchymal transition

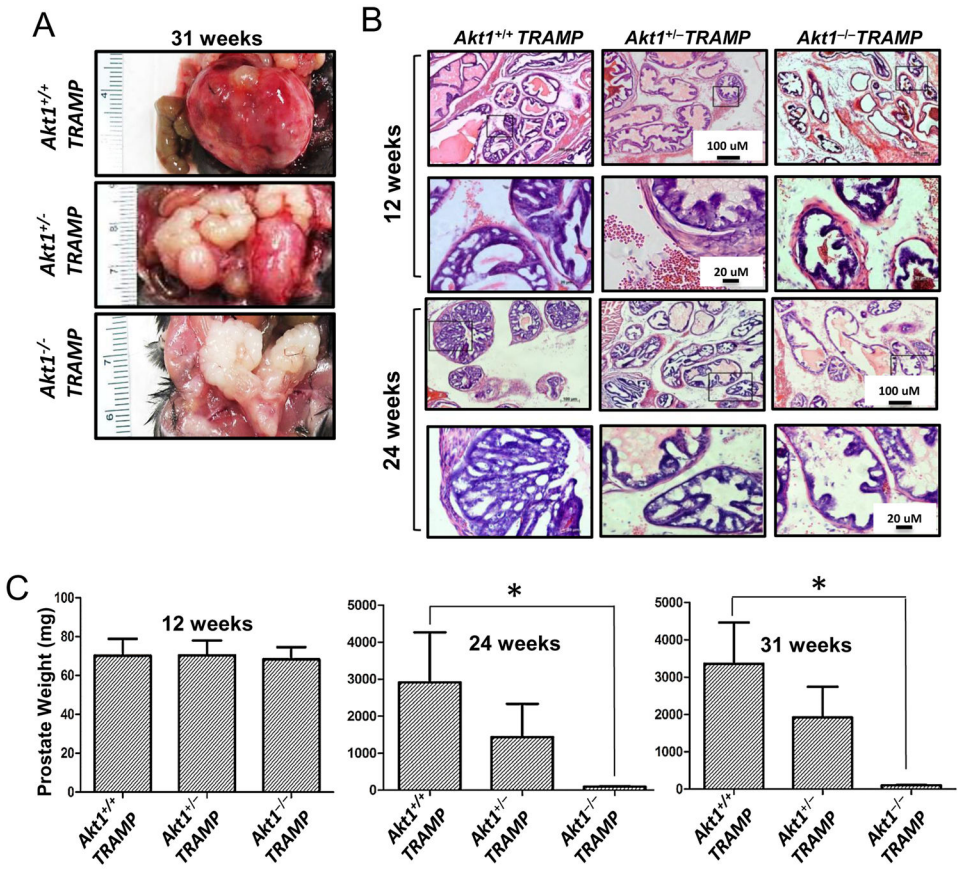

Figure 1. Akt1 deficiency blunts oncogenic transformation in *TRAMP* mouse prostate

(A) Representative images of 31 week old prostate tissues isolated from *TRAMP/Akt1*$^{+/+}$, *TRAMP/Akt1*$^{+/-}$, *TRAMP/Akt1*$^{-/-}$ mice showing significant tumor growth in *TRAMP/Akt1*$^{+/+}$prostate, significant reduction in tumor size in *TRAMP/Akt1*$^{+/-}$, and no signs of a tumor in *TRAMP/Akt1*$^{-/-}$ prostate (n=9). **(B)** Representative images of *TRAMP/Akt1*$^{+/+}$, *TRAMP/Akt1*$^{+/-}$, *TRAMP/Akt1*$^{-/-}$ mice prostate tissue sections showing development of PIN in *TRAMP/Akt1*$^{+/+}$ mice prostates, and the absence of PIN in *TRAMP/Akt1*$^{-/-}$ and *TRAMP/Akt1*$^{+/-}$ mice prostates at 12 weeks of age. Also shown is the presence of high glandular proliferation of the tumor in *TRAMP/Akt1*$^{+/+}$ mice prostates, moderate glandular proliferation of the tumor in *TRAMP/Akt1*$^{+/-}$ mice prostates, and no glandular proliferation of the tumor in *TRAMP/Akt1*$^{-/-}$ mice prostates at 24 weeks of age (n=6). **(C)** Bar graphs showing average weight of *TRAMP/Akt1*$^{+/+}$, *TRAMP/Akt1*$^{+/-}$, *TRAMP/Akt1*$^{-/-}$ mice prostates at 12, 24 and 31 weeks of age (n=9). Data presented as Mean ± SD; *$P < 0.05$.

Figure 2

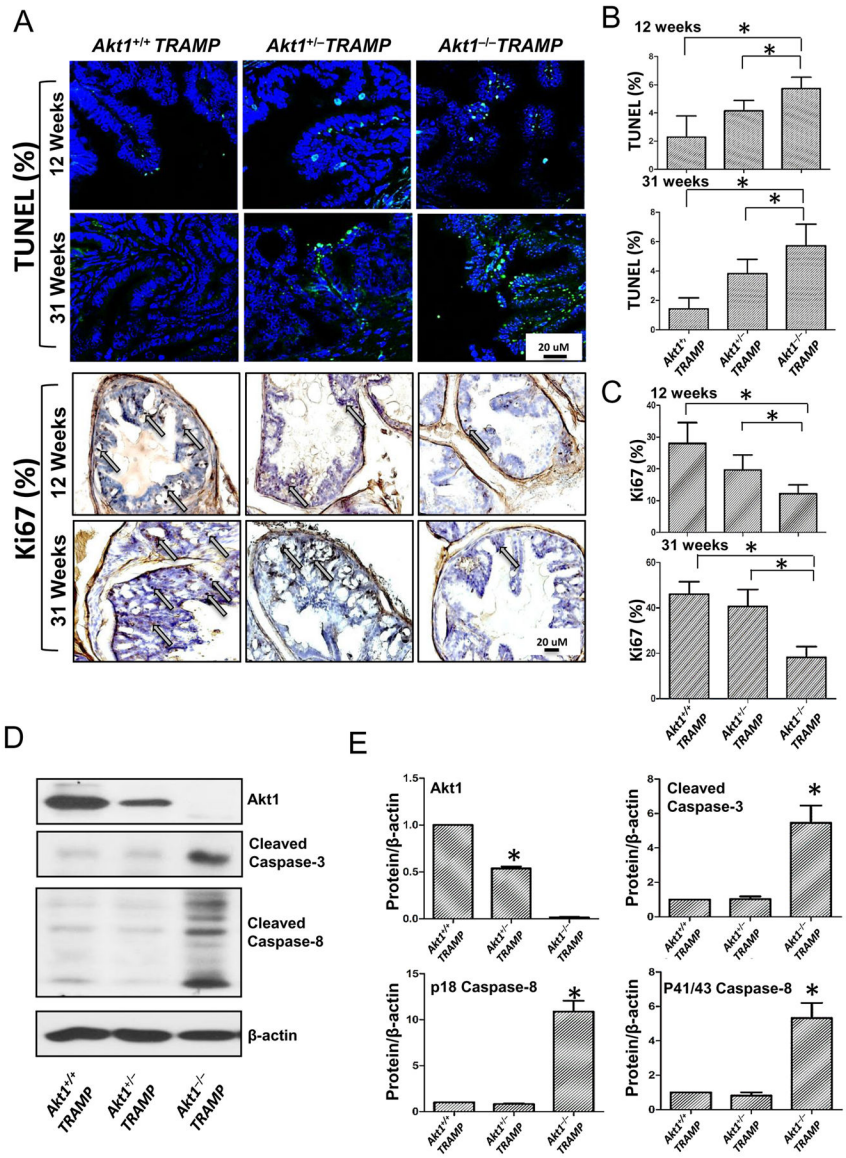

Figure 2. Akt1 deficiency increases apoptosis and inhibits proliferation in TRAMP mouse prostate

(A) Representative images of 12 and 31 week old prostate tissue sections from *TRAMP/Akt1*$^{+/+}$, *TRAMP/Akt1*$^{+/-}$, *TRAMP/Akt1*$^{-/-}$ mice showing TUNEL and Ki67 staining (n=6). **(B)** Bar graphs showing quantification of the TUNEL positive cells in 12 and 31 week old *TRAMP/Akt1*$^{-/-}$ and *TRAMP/Akt1*$^{+/-}$ mice prostates compared to *TRAMP/Akt1*$^{+/+}$ (n=6). **(C)** Bar graphs showing the number of Ki67 positive cells in 12 and 31 week old *TRAMP/Akt1*$^{-/-}$ and *TRAMP/Akt1*$^{+/-}$ mice prostates compared to *TRAMP/Akt1*$^{+/+}$ (n=6). **(D)** Representative Western blot images and **(E)** bar graphs showing expression levels of Akt1, cleaved caspase-3, cleaved caspase-8 and β-actin in 31 week old *TRAMP/Akt1*$^{+/+}$, *TRAMP/Akt1*$^{+/-}$, *TRAMP/Akt1*$^{-/-}$ mice prostate tissue lysates (n=4). Data presented as Mean ± SD; $*P < 0.05$.

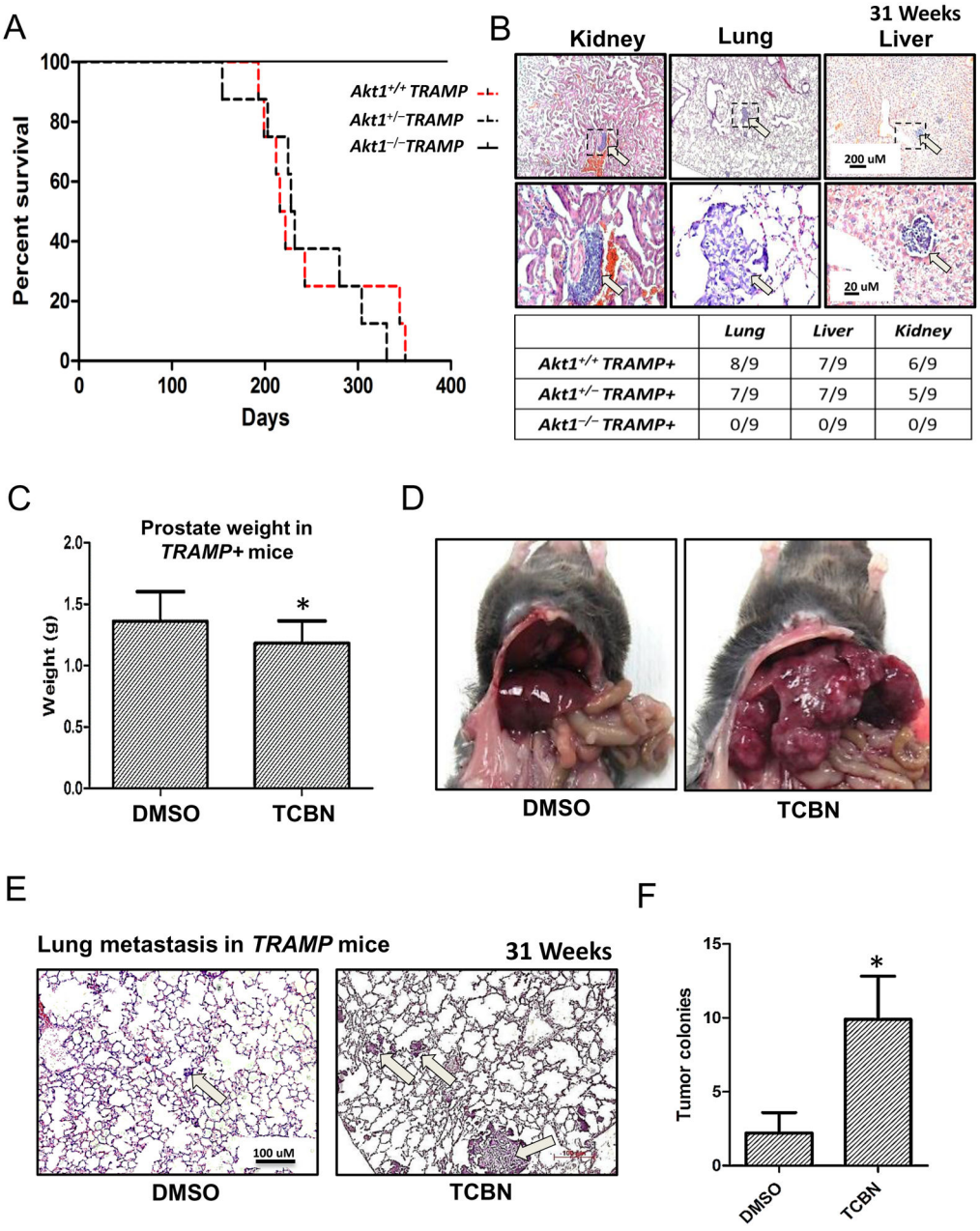

	Lung	Liver	Kidney
Akt1$^{+/+}$ *TRAMP+*	8/9	7/9	6/9
Akt1$^{+/-}$ *TRAMP+*	7/9	7/9	5/9
Akt1$^{-/-}$ *TRAMP+*	0/9	0/9	0/9

Figure 3. Pharmacological inhibition of Akt in 25 week old tumor bearing *TRAMP* mice promotes prostate cancer metastasis to the lungs

(A) Kaplan-Meier plot showing increased lifespan of *TRAMP/Akt1*$^{-/-}$ mice compared to *TRAMP/Akt1*$^{+/+}$and *TRAMP/Akt1*$^{+/-}$ mice (n=12). **(B)** Representative images of 31 week old kidney, lung and liver tissues isolated from *TRAMP/Akt1*$^{+/+}$ mice showing metastatic tumor nodules. Table below indicate total absence of metastatic prostate cancer colonies in either the kidney, lung, and liver in *TRAMP/Akt1*$^{-/-}$ mice, and relatively the same number of metastatic prostate cancer colonies in the kidney, lung, and liver of the *TRAMP/Akt1*$^{+/+}$and *TRAMP/Akt1*$^{+/-}$ mice (n=9). **(C)** Bar graph showing the weight of 31 week old *TRAMP/Akt1*$^{+/+}$ prostate tumor treated for 6 weeks with DMSO (control) or Akt inhibitor

(1mg/kg/day TCBN) (n=6). **(D)** Representative images of 31 week old *TRAMP/Akt1*$^{+/+}$ mice viscera showing metastatic coloies in the livers treated with 1mg/kg/day TCBN for 6 weeks, compared to DMSO controls TCBN (n=6). **(E)** Representative images of 31 week old *TRAMP/Akt1*$^{+/+}$ mice lung sections 6 weeks after treatment with DMSO or 1mg/kg/day TCBN (n=6). **(F)** Bar graph showing significantly higher number of prostate cancer colonies in 6 week TCBN-treated *TRAMP/Akt1*$^{+/+}$ mice lung sections compared to DMSO-treated controls (n=6). Data presented as Mean ± SD; $*P < 0.05$.

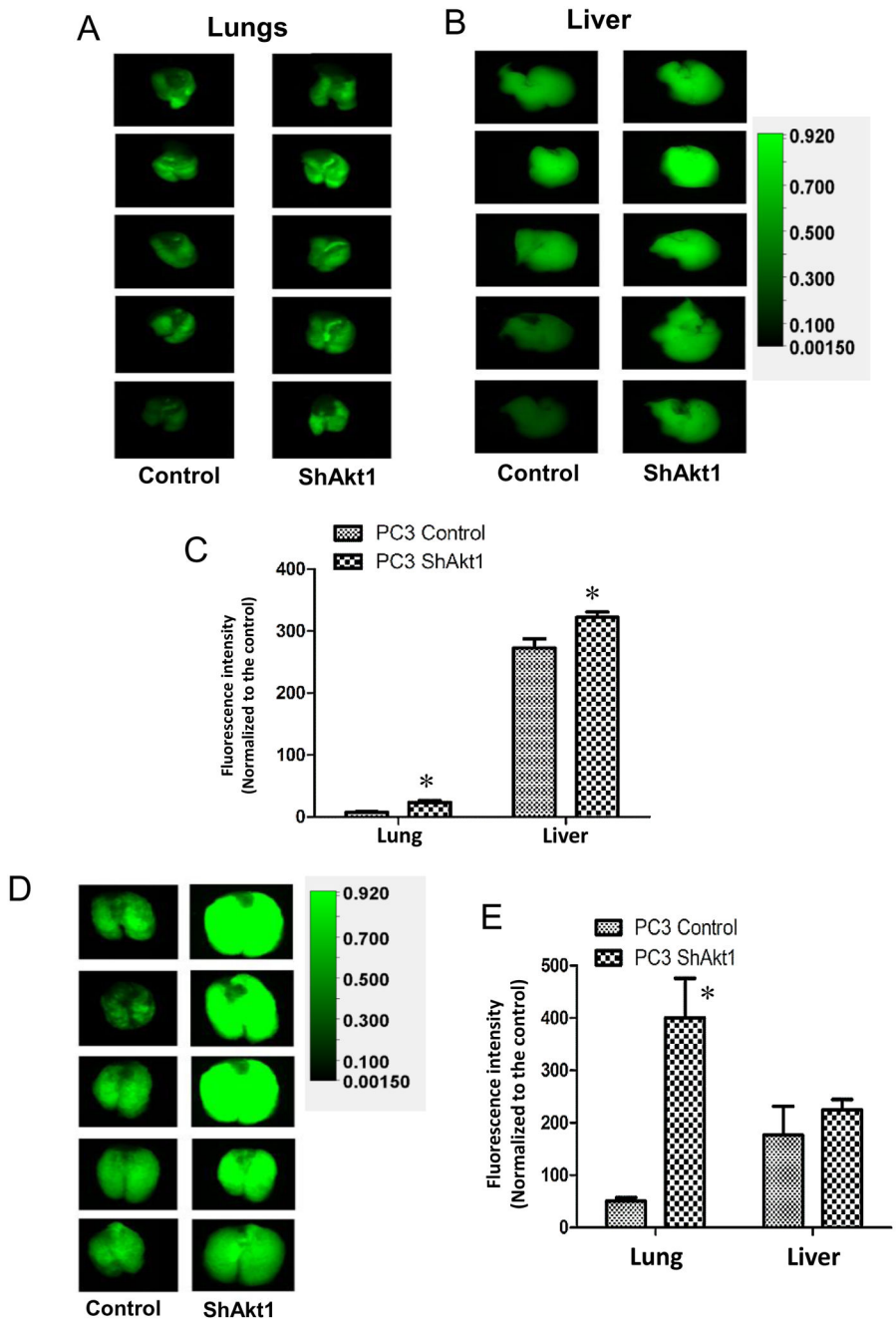

Figure 4. Akt1 loss in human PC3 prostate cancer cells promotes lung metastasis

(A) Representative images of IRDye 800CW 2-deoxy glucose loaded lungs and **(B)** livers from athymic nude mice pre-administered (via tail-vein; 3 days ago) with Control ShRNA (Control) or Akt1 ShRNA (ShAkt1) expressing human PC3 cells. **(C)** Bar graph showing the quantified fluorescent intensity of uptaken IRDye 800CW 2-deoxy glucose by the lungs and liver in athymic nude mice pre-administered with ShControl or ShAkt1 expressing human PC3 cells (n=8). **(D)** Representative images of IRDye 800CW 2-deoxy glucose loaded lungs from athymic nude mice pre-administered (via tail-vein; 2 weeks ago) with ShControl or ShAkt1 expressing human PC3 cells. **(E)** Bar graph showing the quantified fluorescent

intensity of uptaken IRDye 800CW 2-deoxy glucose by the lungs and liver in athymic nude mice pre-administered (via tail-vein; 2 weeks ago) with ShControl or ShAkt1 expressing human PC3 cells (n=8). Data presented as Mean ± SD; *$P < 0.05$.

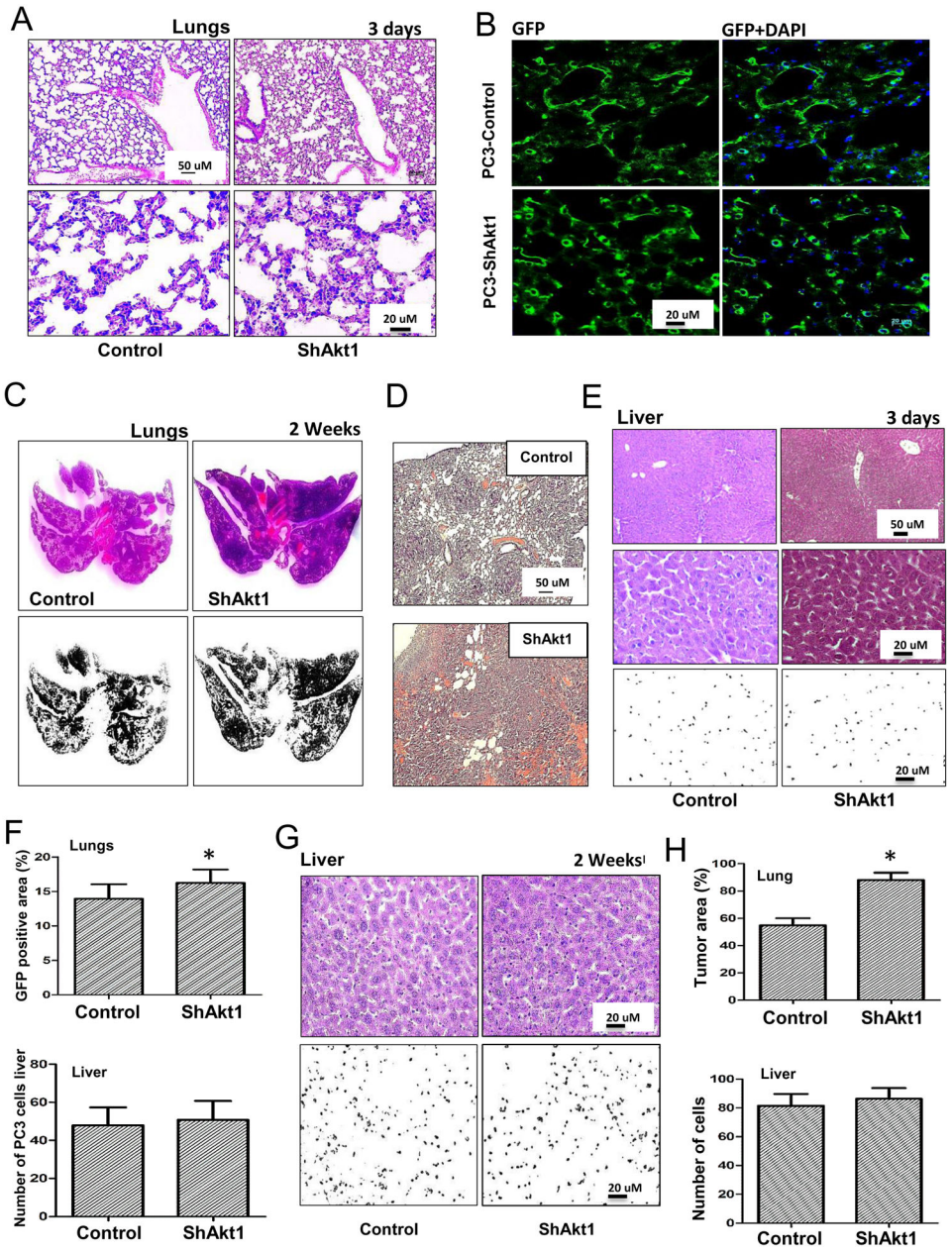

Figure 5. Increased metastasis and lung colonization by Akt1 knockdown PC3 cells compared to control PC3 cells *in vivo*

(A) Representative images of H&E stained lung sections along with binary images from athymic nude mice pre-administered (via tail-vein; 3 days prior to analysis) with control or ShAkt1 PC3 cells. **(B)** Representative images of frozen lung sections from athymic nude mice pre-administered (via tail-vein; 3 days prior to analysis) with GFP-expressing control or Akt1 knockdown PC3 cells. **(C–D)** Representative images of H&E stained and binary images of the lung sections of athymic nude mice pre-administered (via tail-vein; 2 weeks prior to analysis) with Control or ShAkt1 PC3 cells. **(E)** Representative H&E stained and binary images of the liver sections from athymic nude mice pre-administered (via tail-vein; 2 weeks ago) with control or Akt1 knockdown PC3 cells showing increased number of tumor

cells in mice administered with Akt1 knockdown PC3 cells compared to control. **(F)** Bar graphs showing the number of control and Akt1 knockdown GFP-positive PC3 cells in the lung (above) and number of PC3 cells in the binary images of liver sections (below) from athymic nude mice pre-administered with respective PC3 cells 3 days prior to tissue isolation (n=6). **(G)** Representative H&E stained and binary images of the liver sections from athymic nude mice pre-administered (via tail-vein; 2 weeks ago) with control or Akt1 knockdown PC3 cells. **(H)** Bar graphs showing the area of control and Akt1 knockdown PC3 cell tumor colonization in the lung (above) and the number of PC3 cells in the binary images of the liver sections (below) from athymic nude mice pre-administered with respective PC3 cells 2 weeks prior to tissue isolation (n=6). Data presented as Mean ± SD; $*P < 0.05$.

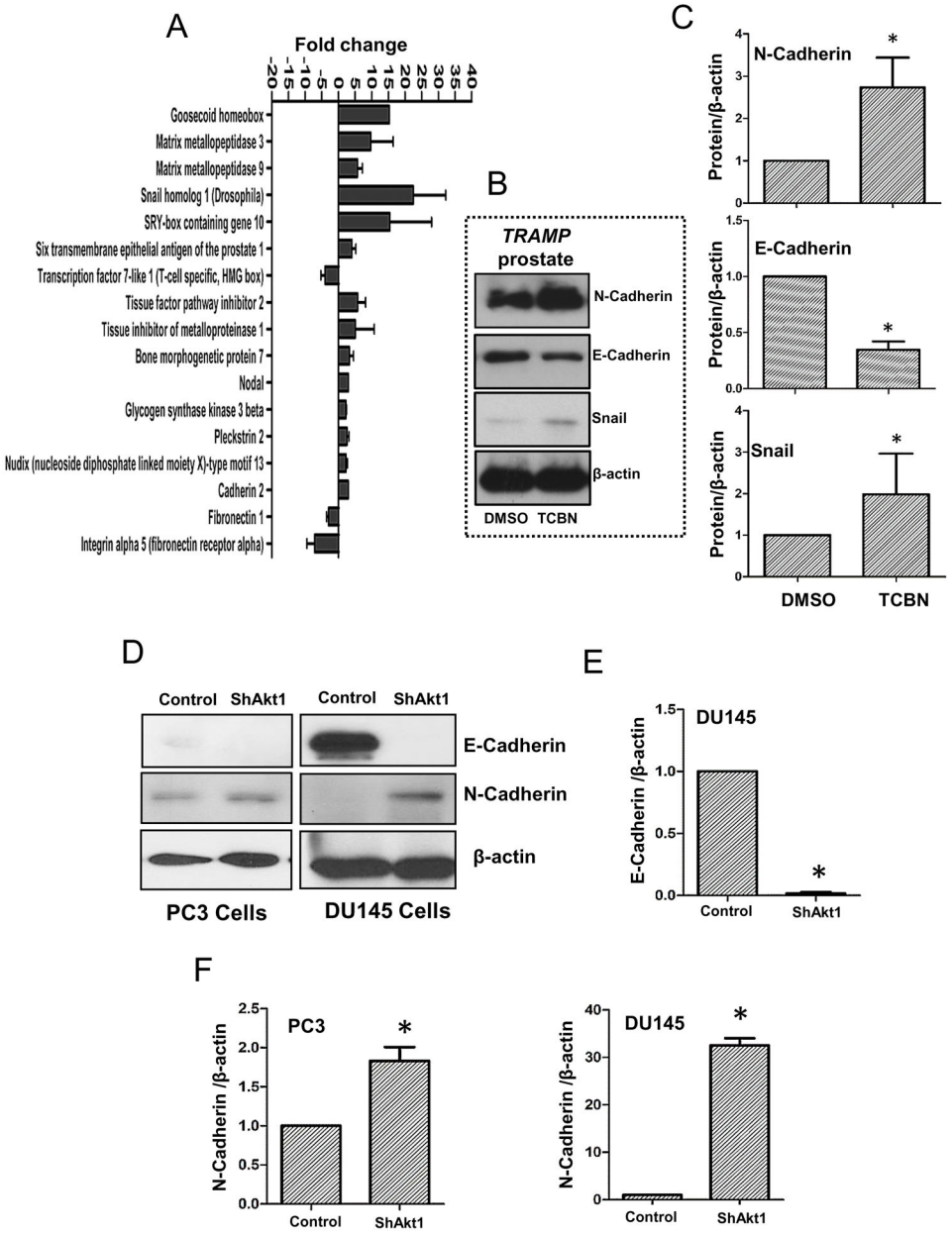

Figure 6. Pharmacological inhibition of Akt in *TRAMP* mice and genetic deletion of Akt1 in human prostate cancer cells promote epithelial to mesenchymal transition (EMT)

(A) Bar graph showing changes in the mRNA expression of genes regulating EMT in 31 week old *TRAMP* mice prostate tissues treated with 1mg/kg/day Akt inhibitor TCBN for 6 weeks (n=3). **(B)** Representative Western blot images of prostate tissue lysates isolated from 31 week old, 6 week TCBN (1mg/kg/day) treated *TRAMP* mice showing changes in the protein expression of epithelial and mesenchymal markers compared to DMSO treated controls. **(C)** Bar graphs showing average fold-changes in the expression levels of mesenchymal markers N-Cadherin and Snail, and epithelial marker E-cadherin in prostate tissue lysates isolated from 31 week old, 6 week TCBN treated *TRAMP* mice compared to DMSO treated controls (n=4). **(D)** Representative Western blot images of Akt1 knockdown

human PC3 and DU145 cell lysates showing changes in the expression levels of epithelial marker E-cadherin and mesenchymal marker N-Cadherin compared to ShControl cells. **(E)** Bar graph showing average fold-change in the expression levels of epithelial marker E-Cadherin in Akt1 knockdown DU145 cell lysates compared to ShControl cell lysates (n=4). **(F)** Bar graphs showing average fold-change in the expression levels of mesenchymal markers N-Cadherin in Akt1 knockdown PC3 (left) and DU145 (right) cell lysates compared to respective control cell lysates (n=4). Data presented as Mean ± SD; $*P < 0.05$.

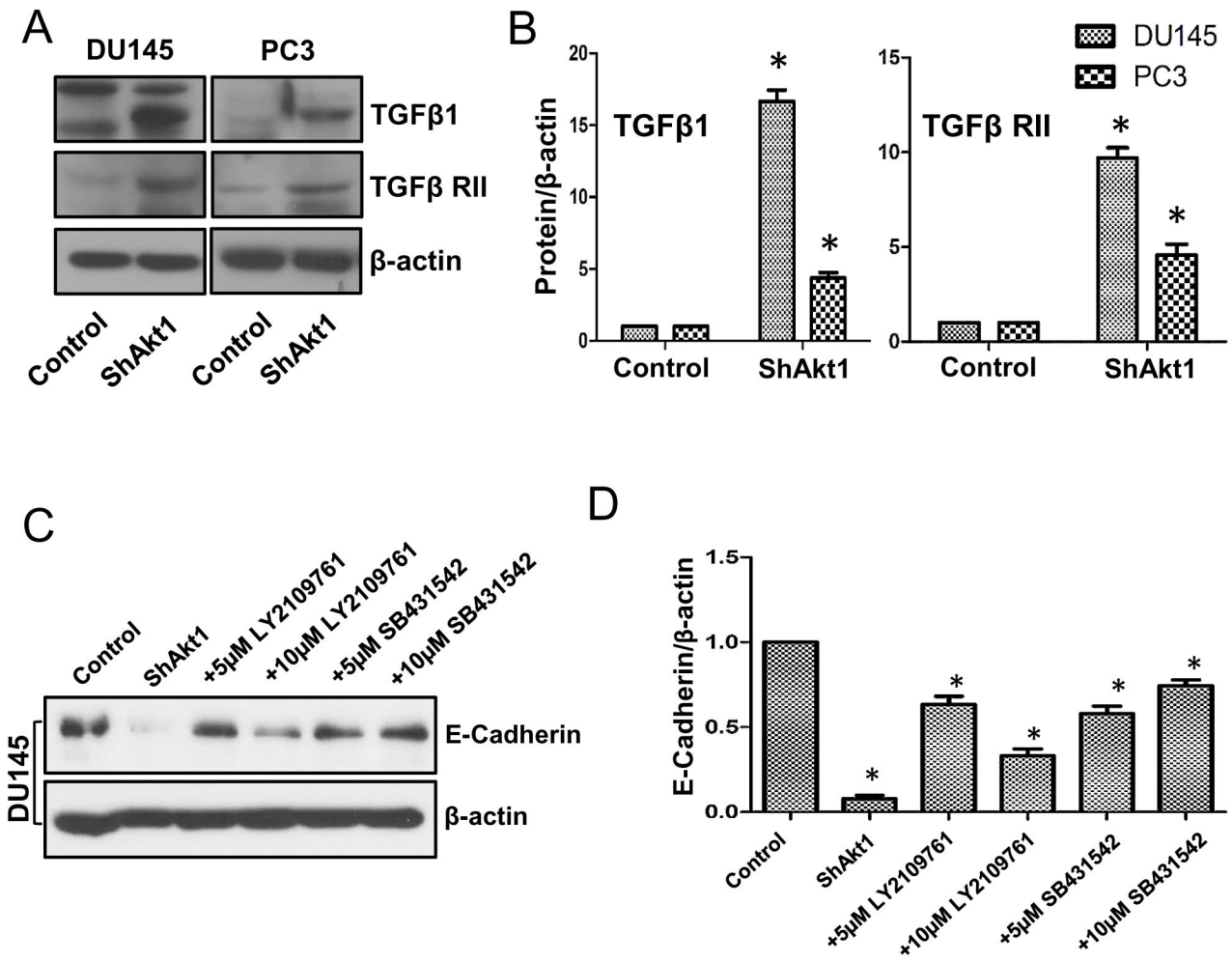

Figure 7. Akt1 suppression in human prostate cancer cells result in increased expression of EMT-inducing growth factor TGFβ1 and its receptor TGFβ RII

(A) Representative Western blot images of control and Akt1 knockdown PC3 and DU145 cell lysates showing changes in the expression levels of TGFβ1 and its receptor TGFβ RII compared to respective control cell lysates. **(B)** Bar graphs showing average fold-changes in the expression levels of TGFβ1 and its receptor TGFβ RII in Akt1 knockdown PC3 and DU145 cell lysates compared to respective control cell lysates (n=4). **(C)** Representative Western blot images of control and Akt1 knockdown DU145 cell lysates showing changes in the expression levels of epithelial marker E-cadherin in the presence and absence of DMSO (control), and various doses of TGFβ receptor inhibitors LY2109761 and SB431542 compared to control cell lysates. **(D)** Bar graphs showing average fold-changes in the expression levels of E-cadherin in Akt1 knockdown DU145 cell lysates treated in the presence and absence of DMSO (control), and various doses of TGFβ receptor inhibitors LY2109761 and SB431542 compared to control cell lysates (n=4). Data presented as Mean ± SD; $*P < 0.05$.

Figure 8

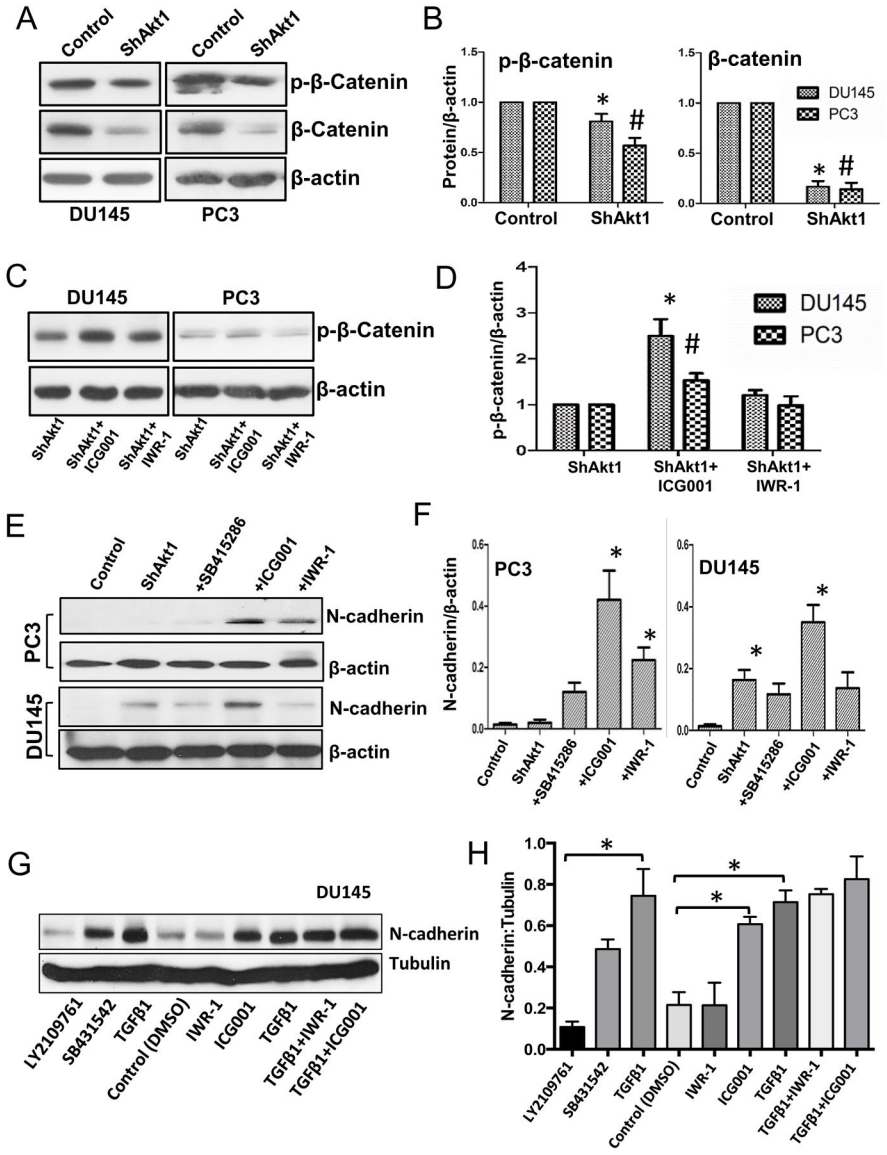

Figure 8. Prostate cancer cell EMT as a result of Akt1 suppression is reliant on reduction in the levels of β-catenin

(A) Representative Western blot images of control and Akt1 knockdown PC3 and DU145 cell lysates showing changes in the expression levels of β-Catenin and p-β-Catenin compared to respective control cell lysates. **(B)** Bar graphs showing average fold-changes in the expression levels of β-Catenin and p-β-Catenin in Akt1 knockdown PC3 and DU145 cell lysates compared to respective control cell lysates (n=4). **(C)** Representative Western blot images of Akt1 knockdown PC3 and DU145 cell lysates showing changes in the expression levels of p-β-Catenin in the presence and absence of β-Catenin transcription inhibitor ICG001 (10 μM) and Wnt signaling inhibitor IWR-1 (10 μM) 72 hours after treatment. **(D)**

Bar graphs showing average fold-changes in the expression levels of p-β-Catenin in Akt1 knockdown PC3 and DU145 cell lysates in the presence and absence of β-Catenin transcription inhibitor ICG001 and Wnt signaling inhibitor IWR-1 (72 hours) (n=4). **(E)** Representative Western blot images of normal PC3 and DU145 cell lysates showing changes in the expression levels of N-Cadherin in the presence and absence of 10 μM of GSK-3 inhibitor SB415286, β-Catenin transcription blocker ICG001 and Wnt signaling inhibitor IWR-1 (72 hours). **(F)** Bar graphs showing fold-changes in the expression levels of N-cadherin in PC3 and DU145 cell lysates pre-treated with GSK-3 inhibitor SB415286, β-Catenin transcription blocker ICG001 or Wnt signaling inhibitor IWR-1 (72 hours). **(G)** Representative Western blot images of DU145 cell lysates showing changes in the expression levels of N-Cadherin after treatment with TGFβ1 (5 ng/ml; 72 hours) alone and in combination with TGFβ receptor inhibitors LY2109761 and SB431542, β-Catenin transcription blocker ICG001 and Wnt signaling inhibitor IWR-1.